Glycosylation Affects the Rate of Traffic of the Shaker Potassium Channel through the Secretory Pathway†

Natalie F. de Souza and Sanford M. Simon*

Laboratory of Cellular Biophysics, The Rockefeller University, New York, New York 10021

Received March 13, 2002; Revised Manuscript Received June 27, 2002

ABSTRACT: We have examined the effect of glycosylation on the traffic of the voltage-gated Shaker potassium channel through the secretory pathway of mammalian cells. Shaker is glycosylated on two asparagines (N259 and N263) in the first extracellular loop. Electrophysiological experiments indicate that glycosylation is not necessary for channel integrity [Santacruz-Toloza et al. (1994) *Biochemistry 33*, 5607]. Consistent with this, we observe that unglycosylated N259Q+N263Q mutant channel forms oligomers as efficiently as the wild type and that this occurs in the endoplasmic reticulum. We have compared the kinetics of secretory traffic of the wild-type glycosylated and the N259Q+N263Q unglycosylated channels. Surface biotinylation of newly synthesized proteins indicates that the rate of delivery of the unglycosylated channel to the cell surface is slower than that of wild type. We have further dissected channel traffic using quantitative imaging. We observe that mutant channel traffics more slowly from the endoplasmic reticulum to the Golgi than wild type at 20 °C. This may contribute to the slowed delivery of the mutant to the cell surface. Neither the surface fraction at steady state nor the stability of Shaker is significantly affected by glycosylation in COS cells.

Shaker is a voltage-gated potassium channel expressed in excitable cells of Drosophila, where it plays a critical role in shaping the action potential and controlling excitability (*1*). The Shaker homologue in mammals consists of a family of voltage-gated channels, Kv1.1-Kv1.6 (*2*). Shaker is a homotetramer, in which each monomer is a polytopic membrane protein with six putative transmembrane domains (*3*−*5*). Although there have been extensive studies on Shaker physiology, there is less understanding of the factors that play a role in its folding, assembly, and traffic (*6*). The channel has been shown to oligomerize in the endoplasmic reticulum (ER) (*7*, *8*). Mutations designed to disrupt Shaker structure or assembly result in channels that do not traffic out of the ER (*9*, *10*). Since Shaker translated in vitro and translocated into ER microsomes shows channel activity, it has been suggested that folding also occurs, at least to some degree, at this location in the secretory pathway (*11*).

N-linked glycosylation is initiated in the ER (*12*). The $Glu_3Man_9GlcNac_2$ core sugar is cotranslationally (*13*) added to asparagine residues on nascent proteins in the context Asn-X-Ser/Thr by the action of the oligosaccharyl transferase (*14*, *15*). The terminal glucose residues of this core moiety are trimmed in the ER, by ER glucosidases I and II. This generates monoglucosylated glycans, which mediate binding of the newly synthesized glycoprotein to the chaperones calnexin/calreticulin (*16*−*18*). The glycoprotein now enters a cycle of de- and reglucosylation and, consequently, a cycle of unbinding and rebinding to calnexin/calreticulin (*16*, *19*−*21*). Properly folded proteins exit this cycle and are exported to the Golgi apparatus, where the carbohydrate is further trimmed and modified, en route to the plasma membrane. Improperly folded proteins are retained in the ER for further cycles of folding (*15*). A certain fraction of proteins fail to fold appropriately and, in a process that is thought to involve ER mannosidase I, are selected for degradation (*22*−*25*).

N-linked glycosylation has been shown to play a role in the biogenesis of a number of membrane proteins, to varying degrees. In some cases, folding and subsequent export from the ER are dependent on glycosylation,for instance, in the nicotinic acetylcholine receptor (*26*, *27*) rhodopsin (*28*), CD4 (*29*), or the high-affinity IgE receptor (*30*). However, there are other proteins, for example, the V1a vasopressin receptor (*31*) and the human choriogonadotropin receptor (*32*), in which traffic has been reported to be independent of glycosylation. The relevance of glycosylation for human physiology is evident in light of diseases that result from aberrations in this process. In long-QT syndrome, lack of glycosylation and consequent ER retention of the HERG channel result in a predisposition to fatal ventricular arrythmia (*33*). In the rare heritable carbohydrate-deficient glycoprotein syndromes, either generalized hypo-N-glycosylation (CDGS type I) or specific loss of *N*-acetyl glycosaminyl transferase II activity (CDGS type II) causes developmental delay and severe neurological dysfunction (*34*). There is no direct implication, to date, of Shaker glycosylation in pathology. However, a mutation that results in aberrant traffic and intracellular retention of its mammalian homologue (Kv1.1) has been linked to human episodic ataxia type-1 (*35*).

† This work was sponsored by NIH Grant EY12346 to SMS.

* Corresponding author. Address: Laboratory of Cellular Biophysics, The Rockefeller University, 1230 York Avenue, New York, NY 10021. Tel.: (212)327-8130. Fax: (212)327-8022. E-mail: simon@rockefeller.edu.

[1] Abbreviations: ER, endoplasmic reticulum; EndoH, endoglycosidase-H; IP, immunoprecipitation; TCA, trichloroacetic acid; BFA, brefeldin A; SDS−PAGE, sodium dodecyl sulfate−polyacrylamide gel electrophoresis; PDI, protein disulfide isomerase; ERGIC, endoplasmic reticulum−Golgi−intermediate compartment; GFP, green fluorescent protein; SEM, standard error of the mean.

10.1021/bi0258041 CCC: $22.00
Published on Web 08/28/2002

The Shaker channel is glycosylated on two asparagines (N259 and N263) in the first extracellular loop. It has been previously demonstrated that mutation of these residues to glutamine (N259Q+N263Q) results in an unglycosylated channel in Xenopus oocytes, HEK293T cells, and Sf9 cells (*36*, *37*). Glycosylation does not appear to be necessary for channel integrity, since electrophysiological experiments indicate that the unglycosylated mutant does form functional channels when expressed in Xenopus oocytes (*36*).

It has recently been shown that the stability of the unglycosylated mutant channel, as well as the surface levels at which it is expressed, are significantly compromised with respect to wild type in HEK293T cells (*38*). Although indicative of an effect of glycosylation on Shaker traffic, these experiments measure steady state levels and therefore do not directly demonstrate such an effect. In a complementary approach, we have examined the kinetics of transport through the secretory pathway of the glycosylated (wild type) and the unglycosylated (mutant) channels. We observe that the rate of delivery of the unglycosylated Shaker channel to the surface of mammalian tissue culture cells is slower than that of wild type. However, we find that, in our experiments, neither the surface fraction at steady state nor the stability of Shaker is significantly affected by glycosylation. Similar behavior has been previously reported for the squid Kv1A channel expressed in Xenopus oocytes (*39*). We have further dissected Shaker channel secretory traffic in mammalian cells to show that the slowed surface delivery of unglycosylated mutant Shaker is at least partially due to slowed export from the ER.

EXPERIMENTAL PROCEDURES

Materials. Unless otherwise specified, all materials were purchased from Sigma Chemical Co (St. Louis, MO). Anti-HA antibodies were purchased from Covance (Richmond, CA), and antibodies to ER markers (anti-PDI and -calnexin) were from Stressgen Biotechnologies (Victoria BC, Canada). The anti-GOS 28 used to mark the Golgi apparatus was a gift from J. Rothman (Memorial Sloan Kettering Cancer Center, NYC). Secondary antibodies used in immunofluorescence were from Jackson Immunoresearch Labs (West Grove, PA); alkaline phosphatase-conjugated secondaries for Western blotting were from Sigma.

Cell culture. COS-1 and HeLa cells (ATCC, Manassas, VA) were maintained in Dulbecco's MEM (Cellgro, Herndon, VA) supplemented with 10% FBS in a humidified incubator at 37 °C and 5% CO_2. For all biochemical experiments, cells were transiently transfected using Fugene6 (Roche, Indianapolis, IN). For imaging experiments, HeLa cells were plated on glass coverslips precoated for 1 h at 37 °C with 50 μg/mL bovine plasma fibronectin (Gibco, Rockville, MD).

Constructs. The N259Q+N263Q mutant Shaker DNA was a gift from D. Papazian. HA tags were generated at the carboxyl terminus of wild-type or mutant channel using standard PCR methods. All PCR products were checked by dideoxy sequencing.

Metabolic labeling, immunoprecipitation, and endo H digestion. Metabolic labeling was typically done at 24−26 h post-transfection. The cells were first incubated in cysteine/methionine/serum-free DMEM for 30 min at 37 °C. Labeling was carried out for 20 min at 37 °C with 0.25 mCi/ml EXPRE^{35}S^{35}Slabel (NEN, Boston, MA) in cysteine/methionine/serum-free media, using 1.2 mL per 6 cm dish. The cells were then chased at 37 °C in DMEM, 10% FBS (or at 20 °C in MEM, 5% FBS), supplemented with 5 mM cysteine/methioine for various times (0−4 h), washed in cold PBS+ (PBS with 2 mM Ca^{2+}, 1 mM Mg^{2+},) and resuspended in solubilization buffer (150 mM NaCl, 50 mM Tris pH 7.5, 1 mM EDTA) with 2% CHAPS, 10mM iodoacetamide, 0.25 mM PMSF, and a protease inhibitor cocktail (Complete, EDTA-free, Roche). Solubilization was carried out for 45 min at 4 °C, and the insoluble material spun away at 19 000*g* for 5 min. Lysates were preincubated with protein A/G sepharose beads (Santa Cruz Biotechnology, Santa Cruz, CA) for 30 min at 4 °C to eliminate nonspecific binding. Shaker-HA was immunoprecipitated by incubating with anti-HA polyclonal antibody overnight and then with protein A/G beads for a further 2 h, both at 4 °C. Beads were washed with 3 mL of solubilization buffer with 1% CHAPS and 1% Triton. The precipitated sample was eluted off the Protein A/G sepharose beads by heating to 100 °C for 5 min in 0.5% SDS, 0.1 M β-mercaptoethanol, and then recovered by centrifugation. Eluted samples were split into two equal aliquots, adjusted to 75 mM sodium citrate pH 5.5 and incubated with or without endoglycosidase H (0.05U/ml)-(Roche), and with protease inhibitors for 12 h at 30 °C. Samples were boiled for 5 min in SDS−PAGE loading buffer, separated by SDS−PAGE and scanned using a Molecular Dynamics Storm Phosphorimager (Amersham-Pharmacia, Piscataway, NJ).

Sucrose density gradient centrifugation. Gradients of 5−20% sucrose in solubilization buffer + 1% CHAPS, 0.25 mM PMSF, were prepared using a Buchler Auto-Densi Flow II C (Haake Buchler Instruments, Saddle Brook, NJ), to a final volume of 11 mL per gradient. Cells were metabolically labeled and solubilized as described above. The lysates were loaded onto a pre-chilled gradient, and spun for 20 h at 36 000 rpm (160 000*g*) in an SW41 Ti rotor (Beckman Instruments, Palo Alto, CA) at 4 °C. The gradients were fractionated and the Shaker-HA was immunoprecipitated out of each fraction as described above.

Surface biotinylation at steady state and Western blotting. Transiently transfected COS cells were rinsed in PBS+, typically 48 h post-transfection, and labeled with freshly prepared 0.5 mg/mL Sulfo-NHS-LC-biotin (Pierce, Rockford, IL) in PBS+ for an hour at 4 °C. The reaction was quenched with Tris, and the samples were washed (X5) in cold Tris-buffered saline. The cells were lysed in solubilization buffer with 1% SDS for 5 min at 100 °C and the insoluble material pelleted. A fraction of the lysate (usually 10%) was removed as the total sample (T) and the rest of the lysate incubated with Softlink avidin beads (Promega, Madison, WI) for 1 h at room temperature. A fraction of the unbound sample equivalent to 10% of starting material was removed (U), and the remaining re-bound to Softlink avidin beads. Beads from both precipitations were washed with 5 mL cold solubilization buffer supplemented with 1% CHAPS, 1% Triton, 0.1% SDS, and the samples were eluted by incubation at 100 °C for 10−12 min (B & B2). Equal fractions of each sample (typically corresponding to 10% of starting material) were run on SDS−PAGE, transferred to PVDF membrane (AmershamPharmacia), probed for Shaker and actin (Sigma), and

visualized using enhanced chemifluorescence (Amersham-Pharmacia). The blots were scanned on a Molecular Dynamics Storm system and quantified using ImageQuant software (both AmershamPharmacia).

Surface biotinylation of newly synthesized proteins. Transfected cells were metabolically labeled as described above and chased for various times (0−3 h). BFA, when added, was present at 5 μg/mL during the chase only. At the end of the chase period, cells were rapidly cooled to 4 °C and then biotinylated as above. After washing in cold Tris-buffered saline (X5), the cells were scraped off and solubilized in 2% CHAPS, and the Shaker-HA were immunoprecipitated. Immune complexes were eluted off the Protein A/G sepharose beads by incubation in elution buffer (50 mM glycine-HCl pH 2.5, 150 mM NaCl, 0.1% Triton) at 4 °C for 10 min (X2). Eluted samples were collected by centrifugation, neutralized with Tris, and then subjected to a second affinity precipitation with Softlink avidin beads (Promega) at 4 °C, to determine the biotinylated fraction. The unbound sample and the first wash were recovered by TCA precipitation. Equal fractions of bound and unbound (the wash was not quantified as preliminary experiments indicated minimal sample in this fraction) were run on SDS−PAGE and the gels scanned as above. Band intensities were quantified using ImageQuant software and the biotinylated fraction calculated as $\{B/(U + B)\}$*100. Both the immunoprecipitation and the avidin precipitation in this experiment were complete, since no material was recovered upon reprecipitation of the supernatant in each case.

Microinjection, ER−Golgi traffic and imaging. To monitor traffic of the Shaker channel from ER to Golgi, we used intranuclear microinjection of cDNA to generate a population of channels that synchronously traversed the secretory pathway. We switched to HeLa cells for these experiments since COS cells proved too sensitive to microinjection. Cells were microinjected using micropipets pulled from borosilicate glass (1 mm outer diameter, 0.78 mm inner diameter) (Sutter, Novato, CA) on a P-87 puller (Sutter). The DNA was diluted to 30 μg/mL in nuclear injection buffer (140 mM KCl, 10 mM Hepes pH 7.4), centrifuged to remove insoluble material, back-loaded into the micropipet, and injected into cell nuclei under constant pressure. Cells were maintained in Hank's Balanced salt solution during the 10 min injection period. Following this, the medium was exchanged for prewarmed DMEM, 10% FBS, and the cells were incubated at 37 °C for 2 h to allow for expression. The medium was then exchanged for precooled (20 °C) MEM, 5% FBS + 50 μg/mL cycloheximide, and the cells were maintained at 20 °C for various times (0−4 h). At the end of each traffic period, the cells were fixed in methanol and stained for Shaker (1:1000 anti-HA mouse monoclonal, 1:200 anti-mouse TexasRed) and for the Golgi apparatus (1:1000 anti-GOS 28 polyclonal, 1:200 anti-rabbit fluorescein). Cells were imaged on an IX-70 inverted microscope (Olympus, Melville, NY) with a 40 X UplanApo lens (N.A. = 1.0). FITC was imaged using an HQ485/10 excitation band-pass, a 505DCLP dichroic, and an HQ515/30 emission band-pass filter (Chroma Technology Corp., Brattleboro, VT). Texas-Red was imaged using a D560/40 excitation band-pass, a 595DCLP dichroic, and a D630/60 emission band-pass filter (Chroma). The fluorescence illumination source was a 150-W xenon lamp (Optiquip, Highland Mills, NY). Images were aquired with a 12-bit Orca-ER cooled CCD (Hamamatsu, Bridgewater, NJ) controlled by our own software written in Labview 5.1 using the IMAQ Vision package (National Instruments, Austin, TX). Image analysis was done using Metamorph software (Universal Imaging, Downington, PA). For wild-type as well as mutant channel, cells with a visible rim-stain were excluded from the analysis to minimize the confounding effect of surface channel on the data. Apart from this criterion, all cells with visually distinguishable signal over background were included in the analysis.

Determination of channel half-time. Transfected COS cells were metabolically labeled as described above and then chased for up to 24 h at 37 °C or up to 4 h at 20 °C. At each time point, cells were solubilized and lysates prepared as described. Equal cpm (determined in triplicate) for each lysate were subjected to immunoprecipitation as described, run on SDS−PAGE, and quantified using ImageQuant (AmershamPharmacia). All statistical analysis was performed with SigmaPlot software (Jandel Scientific, San Rafael, CA).

RESULTS

We have used heterologous expression of wild-type and N259Q+N263Q mutant channels in COS-1 and HeLa cells for our experiments. Both channels have been tagged at the carboxyl terminus with an HA epitope for convenient manipulation. Two-electrode voltage clamp measurements indicate that the epitope tag does not detectably disrupt structure, since the wild-type tagged construct generates functional, voltage-gated channels when expressed in Xenopus oocytes (data not shown). Metabolic labeling (pulse-chase) of transfected COS cells, followed by endoglycosidase H (endo-H) digestion and immunoprecipitation, were used to characterize the wild-type and mutant channel (Figure 1A). In the case of the wild type, a 3 h chase results in the appearance of a higher molecular weight endo H-resistant band and the concomitant disappearance of the lower molecular weight endoH-sensitive band (lanes 1−4), which indicates traffic of this glycosylated protein from the ER to the Golgi. In contrast, the N259Q+N263Q mutant shows no shift in molecular weight after this chase period and is endoH-resistant at all chase times, as one would expect of an unglycosylated protein (lanes 5−8). The channels display essentially the identical profile in HeLa cells (data not shown). This is consistent with the electrophoretic mobility patterns that have been reported in Xenopus oocytes and HEK293T cells (*36, 37*).

The oligomerization state of wild-type and mutant channel expressed in COS cells was assayed by sucrose density gradient centrifugation (Figure 1B). At least some of the mutant would be expected to form normal tetramers since its electrophysiological behavior is normal (*36*). However, two-electrode voltage clamp would not report the presence of additional misfolded channels (such as aggregates of channels) either at the plasma membrane or at intracellular locations. Since tetramerization occurs in the ER and since this is also the site of quality control, we were interested in comparing the channels in their immature ER states. Transiently transfected cells were pulse-labeled for a brief enough period to allow no post-ER traffic (20 min) and solubilized in 2% CHAPS or Zwittergent 3−14. Zwittergent, unlike CHAPS, is known to disrupt the quarternary structure of both

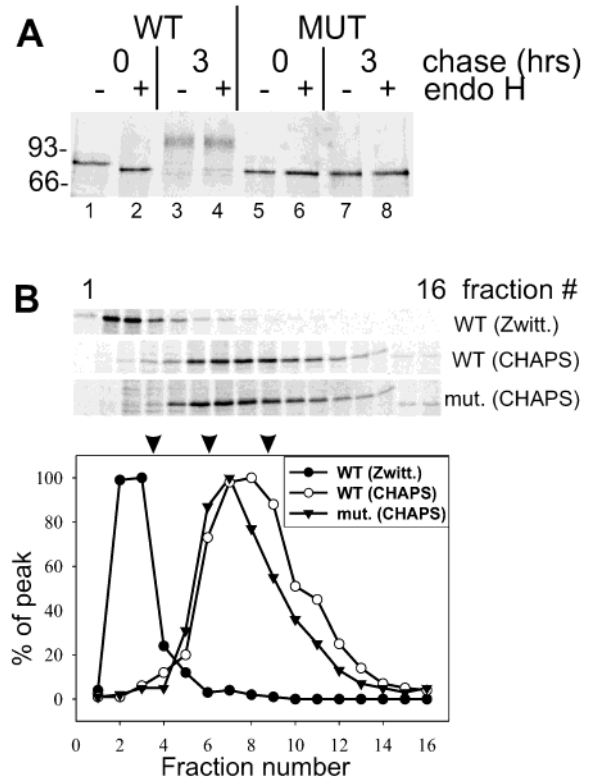

FIGURE 1: Wild-type glycosylated and mutant unglycoslated Shaker channel expressed in COS-1 cells. In panel A, cells transfected with HA-tagged WT or N259Q+N263Q mutant channel were metabolically labeled for 20 min and chased for 0 or 3 h at 37 °C. The cells were lysed in 2% CHAPS and the lysates digested with endoglycosidase H to distinguish between immature (ER) and mature (Golgi) forms of the channel. Shaker was immunoprecipitated using an anti-HA antibody and run on SDS−PAGE. In panel B, CHAPS or Zwittergent lysates of pulse-labeled transfected cells were centrifuged through a 5−20% sucrose gradient. The gradients were fractionated, each fraction subjected to immunoprecipitation with anti-HA and separated on SDS−PAGE. Sucrose density increases with increasing fraction number. The arrowheads above the plot indicate the approximate migration of, from left to right, BSA (66 kD), aldolase (160 kD), and catalase (240 kD).

Shaker and its mammalian counterpart Kv1.1 and render the channels monomeric (*7*, *40*, *41*). The lysates were run on a 5−20% sucrose gradient (Figure 1B). There was no discernible difference between the wild-type and mutant channels. Specifically, there was no indication of increased aggregation of the mutant channel. We conclude that glycosylation plays no significant role in the oligomerization of the Shaker channel, at least as assayed by density gradient centrifugation. This is also true when the channels are translated in vitro and translocated into canine pancreatic microsomes (data not shown). Both the lighter and the heavier peaks of wild-type Shaker migrate slightly smaller than expected. At ∼72 kD, the glycosylated monomer would be expected to comigrate with BSA (66 kD), whereas the ∼ 300 kD tetramer should be slightly larger than catalase (240 kD). It is possible that the sedimentation properties of Shaker are slightly different from those of the marker proteins used. Significantly, detergents known to distinguish between the monomeric (as observed previously in Zwittergent) and the tetrameric (as observed previously in CHAPS) states of the Shaker channel result in peaks (Figure 1B) that, relative to each other, migrate in a manner consistent with tetramerization.

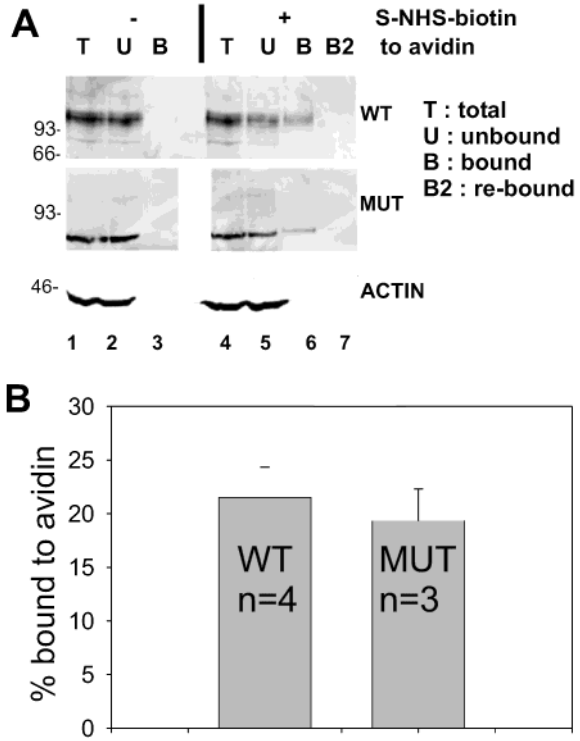

FIGURE 2: Steady-state surface biotinylation of Shaker in COS cells. In panel A, cells transfected with wild-type or N259Q+N263Q mutant channel were labeled at 4 °C with Sulfo-NHS-LC-biotin, washed, and lysed and the lysate then bound to avidin beads. To ensure that the avidin precipitation was complete, unbound material was re-incubated with avidin beads. Equal fractions of the total (T), unbound (U), bound (B) and re-bound (B2) samples were run on SDS−PAGE, transferred to PVDF, and probed for wild-type Shaker-HA (upper panel), mutant Shaker-HA (middle panel) or actin (lower panel). In panel B, the fraction bound {(B/T)*100} is plotted for each channel ($n = 4$ for WT, $n = 3$ for mutant; data represent mean ± SEM).

We next compared the glycosylated and unglycosylated channels in terms of their rate of delivery to the cell surface. To exclusively label surface proteins, we made use of a membrane impermeant, primary amine-directed biotinylating agent (Sulfo-NHS-LC-biotin). We first tested if this reagent is indeed membrane-impermeant under the conditions of our experiment (Figure 2A). Upon surface biotinylation a fraction of both wild-type (upper panel) and mutant (middle panel) Shaker, but not of cytosolic actin (lower panel), can be precipitated by avidin beads. This precipitation depends on biotinylation, and is therefore specific (compare lanes 3 and 6). Moreover, reprecipitation of the unbound fraction (lane 7) indicates that the precipitation is complete, since there is no further material recovered. The mean surface fractions of wild-type and mutant channel measured 48 h post-transfection are plotted in Figure 2B and are not significantly different from each other.

The rate of surface delivery of the two channels was quantified using surface biotinylation at various chase times after a pulse of radioactive cysteine/methionine (Figure 3). We employed a double precipitation protocol, in which the radiolabeled channel was first immunoprecipitated out of a CHAPS lysate, then eluted from the protein A-sepharose at low pH, and then reprecipitated with avidin to determine the biotinylated fraction. The unbound and bound fractions (precipitation 2) from a few time points of representative

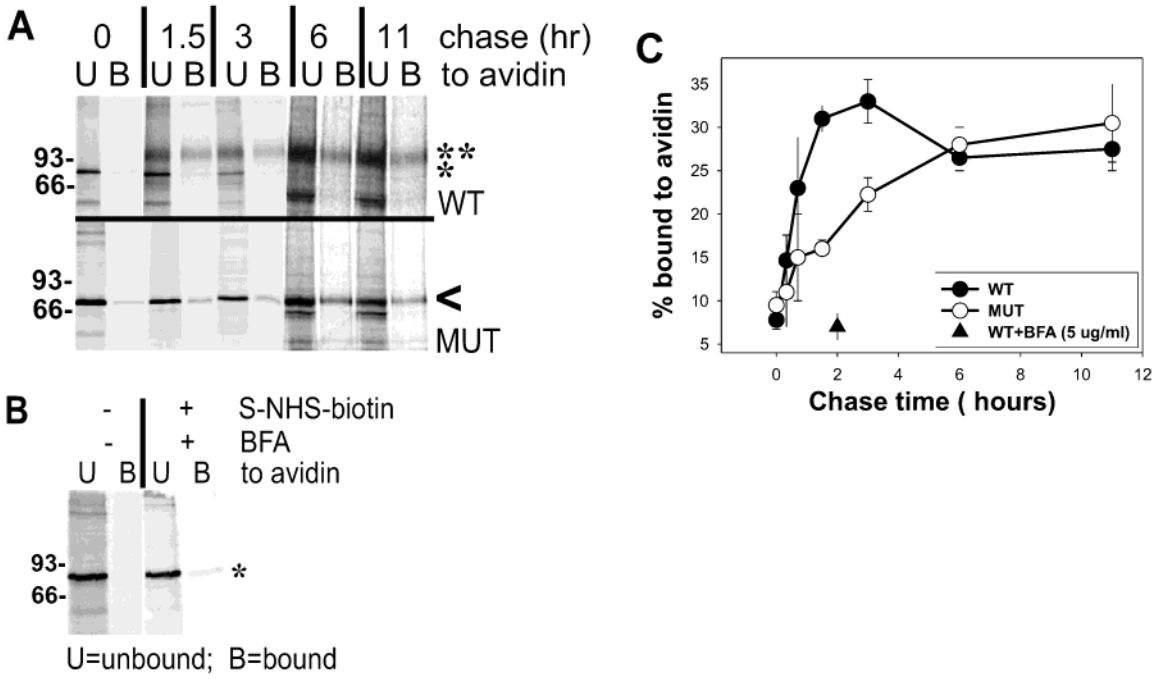

FIGURE 3: Surface biotinylation of newly synthesized Shaker channel in COS cells. COS cells transfected with WT or N259Q+N263Q mutant channel were metabolically labeled for 20min, chased for various times, and biotinylated at 4 °C with Sulfo-NHS-LC-biotin. The channel was immunoprecipitated, eluted off the protein-A beads using a glycine buffer, pH 2.5, and then affinity precipitated with avidin beads to determine the biotinylated fraction. The TCA precipitated unbound material **U** and the avidin-bound material **B** from this second precipitation were run on SDS−PAGE. A selection of time points from representative experiments have been shown for wild-type (upper panel) and mutant (lower panel) Shaker. For clarity, the relevant bands have been indicated as follows (WT immature, *; WT mature, **; mutant, <). In the data shown, samples from the two last time points (6 and 11 h) were run on separate gels. The increased background is due to channel degradation during the chase period, which results in reduced signal. In panel B, the above protocol was carried out in the absence of biotinylating agent or on wild-type-transfected cells that had been treated with BFA during the chase period to prevent traffic of the channel through the secretory pathway. In panel C, the biotinylated fraction ($B/\{U + B\}$)*100 has been plotted over time ($n = 5$ for time points at 0−3 h, $n = 2$ for time points > 3 h; data represent mean ± SEM).

experiments are shown in Figure 3A. The signal in the bound fraction initially increases (0−3 h) for both the wild-type (upper panel) and the mutant (lower panel) channel, which is what would be expected as the channel traffics through the secretory pathway to the cell surface. Quantification of data from three independent experiments shows that the rate and extent of surface biotinylation was markedly higher in the wild-type channel as compared to that in the mutant, at chase times of 1.5−3 h (Figure 3C). In experiments on HeLa cells, a similar trend was seen (data not shown).

At longer chase times, however (6−11 h; Figure 3A,C), there is no longer a measurable difference between the fraction of wild-type and mutant channels on the surface. This is consistent with the data presented previously (Figure 2), in which mean surface fractions measured at steady state were not distinguishable for the two channels. If brefeldin A, which blocks traffic through the secretory pathway, was included during the chase period, the biotinylated fraction of wild type at 2 h of chase was at background levels (Figure 3B,C). This strongly suggests that the experiment does indeed report on Shaker traffic through the secretory pathway to the cell surface. Moreover, when we assessed the avidin-bound fraction of radiolabeled actin, it was found to be vanishingly small at all chase times (<0.1%, data not shown). This further confirms that the biotinylation is surface-specific throughout the course of the experiment.

We set out to identify the step in Shaker traffic that is affected by glycosylation. The observation that the fraction of glycosylated channel at the surface increases more quickly than that of the nonglycosylated channel could be attributed to faster transport through the secretory pathway. Delivery to the cell surface may be crudely broken down, in traffic terms, into ER−Golgi and Golgi−plasma membrane traffic. Exit from the ER is often a rate-limiting step in transport of membrane proteins through the secretory pathway, since it is the location at which folding and quality control of secreted and membrane proteins occurs (*15*, *42*). Thus, this was the transport step we examined.

Standard biochemical assays for ER-to-Golgi traffic rely upon changes in glycosylated moieties as the protein moves through the secretory pathway. Since this was not possible for the unglycosylated mutant channel, we used quantitative imaging to compare ER-to-Golgi traffic rates of wild-type and mutant Shaker. This is schematically depicted in Figure 4A. Intranuclear microinjection of cDNA was used to generate a synchronous population of cells expressing either wild-type or mutant channel. Injection was limited to a period of 10 minutes to maximize synchronicity. The cells were then incubated at 37 °C for 2 h to allow for expression of the channel. This expression time was the shortest possible, balancing the requirement for a reasonable signal against that for minimal traffic out of the ER. After this period, cells were treated with cycloheximide to inhibit further protein synthesis and shifted to 20 °C to block any post-Golgi traffic. The cells were allowed to traffic at 20 °C for various times (between 0 and 4 h), after which they were fixed, stained, and imaged. In all cases, the channel was imaged by immunofluorescence staining using a monoclonal antibody

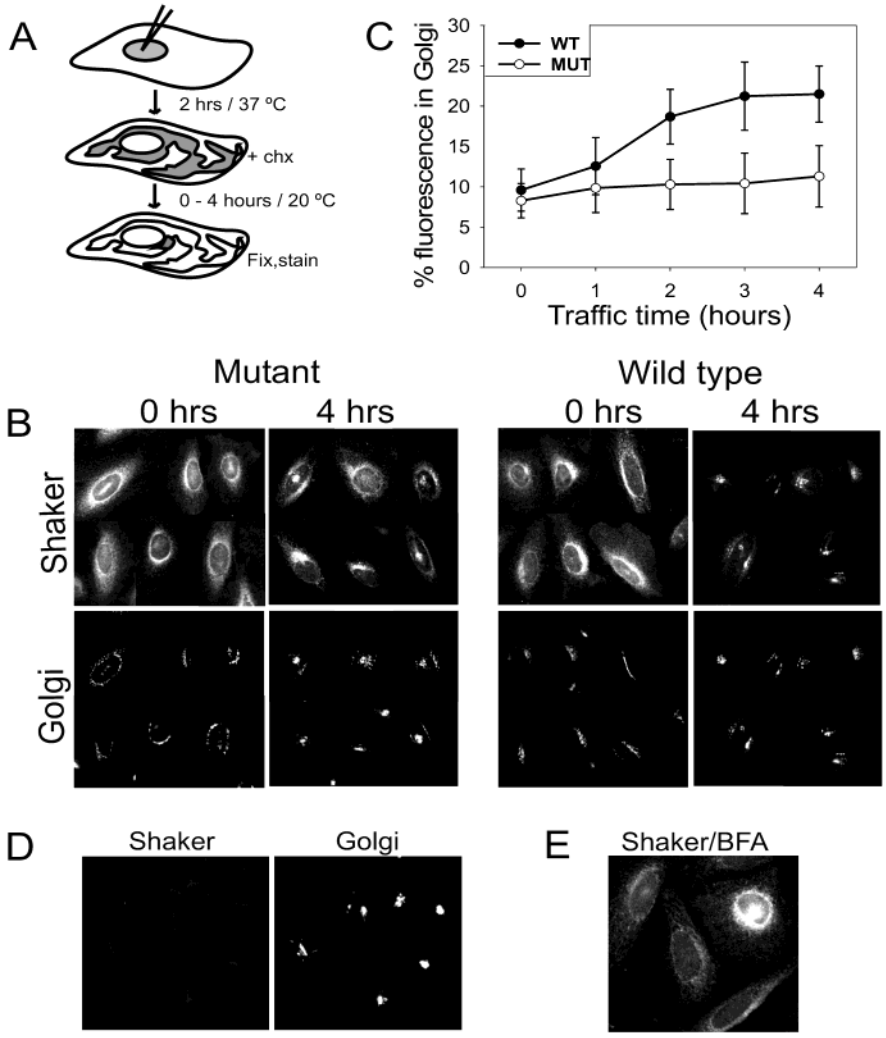

FIGURE 4: ER-to-Golgi traffic of Shaker in HeLa cells. The experiment is schematically depicted in panel A. In brief, WT or N259Q+N263Q mutant Shaker cDNA was microinjected into the nuclei of HeLa cells, expression was allowed to proceed at 37 °C for 2 h, and then cycloheximide was added to prevent further protein synthesis. The cells were chased at 20 °C for 0−4 h, fixed in methanol, stained for Shaker (anti-HA) and Golgi (anti-GOS 28), and imaged by epifluorescence and the fraction of Shaker fluorescence co-localizing with the Golgi determined, for each cell. The 0 and 4 h time points of such an experiment have been shown in panel B. Each panel is a composite to show as many cells as possible. The upper row represents the Shaker channel (display properties are identical for all images), and the lower row represents the corresponding Golgi image in each case. In panel C, the mean (± S.D.; $n = \sim 40$ cells) Golgi fraction has been plotted over time for wild-type (closed circles) and mutant channel (open circles). In panel D are shown uninjected cells stained for Shaker and Golgi. In panel E, cells injected with wild-type Shaker DNA were allowed to traffic for 3 h at 20 °C in the presence of 5 μg/mL BFA and then stained for Shaker.

against the carboxy terminal HA tag. The Golgi apparatus was stained with affinity-purified polyclonal antibody to GOS 28, a Golgi SNARE with a fixed distribution throughout the cis-, medial-, and trans-Golgi (*43*, *44*). The rate at which wild-type and mutant channel moved from ER to Golgi was compared.

The images shown (Figure 4B) are taken from the beginning and end-point of such an assay of the kinetics of transport for wild-type and mutant channel. For both wild-type and mutant Shaker, the fluorescence pattern shifts from more diffuse and reticular to more localized and perinuclear, over time. Moreover, the perinuclear Shaker fluorescence at later times co-localizes with Golgi fluorescence (shown in the lower row, in each case). It is qualitatively evident from these images (Figure 4B) that the residual reticular non-Golgi stain after 4 h of traffic is consistently higher in cells that express the unglycosylated mutant channel when compared to cells expressing the wild type. We have used antibodies against an ER resident protein (calnexin) to stain cells at both early (Figure 5, upper panel) and late (Figure 5, lower panel) traffic times to determine that the reticular pattern seen does indeed colocalize with the ER. This indicates that, as is expected for a membrane protein, the channel moves from an ER to a Golgi location over time, but that this traffic is incomplete over 3−4 h at 20 °C. Co-staining of Shaker with other ER resident proteins (PDI, calreticulin) gave indistinguishable results (not shown).

To quantitatively compare ER−Golgi traffic of the wild-type and mutant channel, we determined the fraction of Shaker fluorescence that co-localizes with the Golgi at various traffic times after addition of cycloheximide and shift to 20 °C. For each cell, the signal in the Golgi fluorescence channel was used to delineate the boundary of the organelle, and the Shaker fluorescence intensity in this area was quantified relative to the total Shaker fluorescence intensity in the same cell. Quantification of ~40 cells for each time

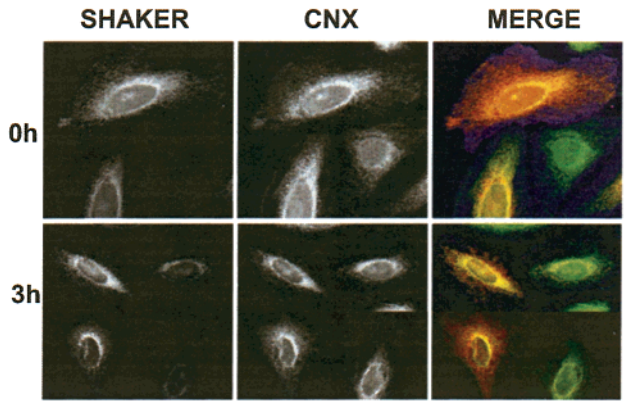

FIGURE 5: HeLa cells were intranuclearly microinjected with cDNA for WT Shaker, incubated for 2 h at 37 °C to allow for expression, chased for 0h (upper panel) or 3h (lower panel) at 20 °C, fixed, and stained for Shaker (α-HA, red in merge) or ER (α-CNX, green in merge).

point is shown (Figure 4C). For each plot, the fraction of Shaker fluorescence in the Golgi area is shown over time. Although there is some increase in the Golgi fraction for the mutant channel, it is clear that the rate at which it traffics from ER to Golgi is markedly slower than that of the wild type, at 20 °C.

Staining of uninjected cells (Figure 4D) shows that there is no bleedthrough from the Golgi into the Shaker fluorescence signal. Morover, if BFA is included during the 20 °C chase period, wild-type channel remains largely reticular after 3−4 h of traffic (Figure 4E).

To test the extent to which Shaker fluorescence that co-localizes with the Golgi does indeed represent protein that has trafficked to the Golgi, we performed the identical analysis on cells that had been only stained for marker proteins of ER and Golgi. This would determine the fraction of a protein in the ER that is reported, by this method, to colocalize with the Golgi. This was found to be 5% (± 2, $n = 13$) for the resident ER protein PDI. Since the fraction of Shaker fluorescence that co-localizes with the Golgi at later traffic times (Figure 4C) is significantly higher, we conclude that we are measuring fluorescence from Shaker that has, indeed, trafficked to the Golgi and is not merely juxtaposed to it. Moreover, the mean fractional Golgi signal that was reported for uninjected cells that had been stained for Shaker and Golgi was also 5% (± 1.5, $n = 11$). This latter signal is the overall background of the experiment and would be a sum of cellular autofluorescence (which tends to be slightly higher in the perinuclear region than in the rest of the cell), any bleedthrough from the Golgi channel, and nonspecific fluorescence background. The fraction of an ER resident protein that is reported to co-localize with the Golgi, therefore, is at background levels.

Last, we carried out pulse-chase experiments to monitor traffic of the wild-type channel from ER to Golgi at 20 °C in HeLa cells (Figure 6). Although the presence of a background band (see lanes 1−3) close to the Shaker bands of interest made quantification difficult, the estimated Golgi fraction (30% ± 7 (S.D.); $n = 3$) is roughly comparable to that measured by the imaging experiment, over a 4 h chase period. We conclude that unglycosylated mutant Shaker traffics more slowly from ER to Golgi than wild type, at 20 °C. We would predict that at least part of the observed difference in the surface delivery rate of the two channels stems from a difference in their ER-to-Golgi traffic.

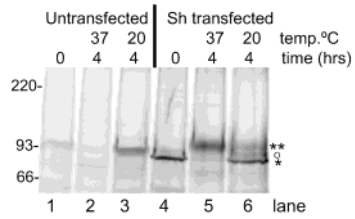

FIGURE 6: Pulse-chase of Shaker channel at 20 °C in HeLa cells. HeLa cells transfected with WT channel (lanes 4−6) were metabolically labeled for 20 min and either not chased (lane 4) or chased for 4 h at 37 °C or 20 °C. The cells were lysed in 2% CHAPS and the channel immunoprecipitated using an anti-HA antibody. The immature ER (*) and mature Golgi (**) forms of the channel are indicated. The faint band (o) between the two Shaker bands is nonspecific background, as it is consistently seen in pulse-chase experiments on untransfected cells. Untransfected cells that have been identically processed have been shown for comparison (lanes 1−3).

Since significant differences in stability of the wild-type and mutant channel could confound comparisons of surface or Golgi fractions, we compared the degradation of the two channels under the conditions in which our experiments were done. The stability of wild-type and mutant channel was compared over 24 h at 37 °C in COS cells (Figure 7A,B) and was found to be very similar. Since our experiment to measure initial rates of surface delivery was terminated at 11 h, it is reasonable to conclude that the relative stability of the channels does not contribute to the perceived difference in surface delivery. There was no significant difference between stability of the wild-type and mutant channel over 4 h at 20 °C in HeLa cells (Figure 7C).

DISCUSSION

The overall structure of the Shaker channel is not grossly disrupted by the elimination of glycosylation in the N259Q+N263Q mutant (*36*, *37*). We have shown here that the resulting unglycosylated channel traffics more slowly to the surface of COS cells. The surface fraction of wild-type channel is approximately double that of the mutant after 2 h of traffic at 37 °C. In contrast, we are unable to measure a significant difference in the surface fraction of wild-type and mutant channel at steady state. It is possible that the mutant channel eventually reaches similar surface levels in COS cells, albeit more slowly than the wild type. Experiments that extend our kinetic analysis to later time points (11 h) indicate that this is indeed the case. Aplysia Kv1 (sqKv1A) channels that have been rendered unglycosylated by mutation show a similar retardation in initial arrival at the surface of Xenopus oocytes, whereas the steady-state surface levels, determined electrophysiologically, are indistinguishable from wild type (*39*). Given the sequence similarity (*45*) of the Drosophila and Aplysia channels, the identical location of the glycosylation site, and the very similar consequences of mutating this site for traffic of either channel, it is reasonable to suggest that the sqKv1A channel is also retarded in the ER−Golgi traffic step. It is worth noting that the experiment in oocytes was done at a lower temperature than that in mammalian cells (20 °C vs 37 °C). If the basis for slower surface delivery of the squid and fly channels is indeed the

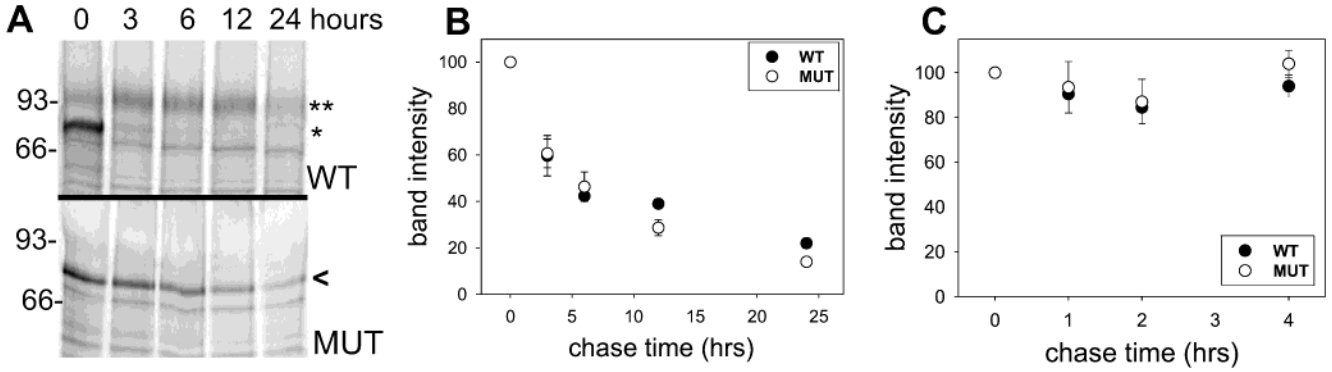

FIGURE 7: Stability of the Shaker channel. In panel A, COS cells transiently transfected with plasmid encoding Shaker were metabolically labeled for 20min and chased for up to 24 h at 37 °C. Lysates were prepared at each time point, and equal cpm of each sample were subjected to immunoprecipitation and then separated on SDS−PAGE. A representative experiment is shown here, for wild-type (upper panel) and N259Q+N263Q mutant (lower panel) Shaker. For clarity, the relevant bands have been indicated as follows (WT immature, *; WT mature, **; mutant, <). In panel B, the band intensities in such an experiment have been quantified and plotted over time ($n = 3$; data represent mean ± SEM). The band intensity at 0 h is taken as 100% for each experiment. The graphs in panel C represent a stability comparison in HeLa cells ($n = 2$; data represent mean ± SEM). Metabolically labeled cells were chased for up to 4 h at 20 °C to simulate the conditions of the imaging experiment.

same, then it appears that the putative folding defect of the unglycosylated channel is not completely rescued at lower temperature. This is consistent with the fact that, as discussed later in this section, we measured a difference between wild-type and mutant Shaker traffic in the early secretory pathway at 20 °C.

All other rates being equal, since WT and NQ channels are delivered to the cell surface at different initial rates, there should theoretically be a difference in the steady state surface fraction in our experiments. Speculatively, similar surface levels of WT and NQ Shaker could be the result of a compensatory difference in endocytic or recycling rates. Further experiments are needed to test this. Although the oligosaccharide groups are topologically extracellular, there is precedent for transmembrane lectin-mediated regulation of glycoprotein traffic to the cell surface. Specifically, interactions with transmembrane lectins have been suggested as a mechanism for targeting glycosylated proteins to the apical surface of polarized cells (*46*, *47*).

In contrast to our results, others have reported a 5−7-fold decrease in the surface fraction of unglycosylated Shaker relative to wild type in HEK293T cells (*38*). It is not clear why the results differ. It is possible that the cell line (COS versus HEK) and/or the biotinylating agent (lysine-directed vs cysteine-directed) affect(s) the outcome of the experiment. Traffic kinetics were not measured in the previous report, but it is not implausible that slowed traffic of mutant Shaker affects its steady state surface level to a greater or lesser degree, depending on the cell type. The surface level of a protein depends on the relative rates of several processes, including surface delivery via the secretory pathway, surface delivery via the recycling pathway, internalization from the cell surface, and degradation. The kinetics of one or more of these additional traffic steps could be differentially affected in wild-type and unglycosylated mutant Shaker, and this could theoretically occur to a different extent depending on the cell type.

We compared the stability of the wild-type and mutant channels over 24 h in COS cells. There is little or no destabilization of unglycosylated Shaker in COS cells, in contrast to data obtained previously in HEK293T cells (*38*), where unglycosylated mutant channel was more rapidly degraded than wild type. Moreover, the degradation was seen to be lactacystin-sensitive and brefeldin A(BFA)-insensitive, suggesting that it occurred in the cytosolic proteasome, directly from the ER. Again, it is possible that the difference in cell line in our experiments contributes to the differing results. For instance, cell-type dependent endogenous expression of putative accessory proteins could influence the stability of the channel either at the cell surface or within an intracellular organelle. Glycosylation-dependent stabilization of the Shaker channel at the cell surface of HEK293T cells, but not COS cells, would be consistent with the difference in our results. Further experiments using more homologous systems will most likely be required in order to fully understand what regulates cell surface levels of the Shaker channel. Importantly for our own experiments, the negligible effect of glycosylation on channel stability means that differential stability is unlikely to make an artifactual contribution to the measured difference in surface delivery rates.

To further our studies, we attempted to identify which step in channel traffic is affected. N-linked glycosylation is initiated in the ER, with further enzymatic modification of the core moiety occurring in both the ER and the Golgi. Although it is known that inhibition of glycosylation can affect ER export of secreted proteins, presumably as a result of misfolding and consequent retention by ER quality control, the effect of glycosylation varies depending upon the protein being studied. Unglycosylated Shaker is transported out of the ER, but we hypothesized that this may take place at a slower rate than in the case of wild-type channel. We have used an approach that employs intranuclear microinjection of cDNA, combined with quantitative imaging of channel traffic, to test this hypothesis. We find that ER-to-Golgi traffic is indeed slower in mutant unglycosylated than in wild-type channel.

The value of intranuclear microinjection, as the method of DNA introduction into the cell, is that a synchronously expressing population of cells can be generated. Combined with the possibility to block protein synthesis after a certain expression period and to restrict post-Golgi traffic (with the 20 °C temperature block), this makes it possible to study a synchronously synthesized population of protein as it traffics

through the early secretory pathway. Quantitative kinetic imaging is more often used to study traffic of GFP-tagged proteins in live cells. Our attempts to do this were thwarted by the fact that GFP fused to the carboxyl terminus of Shaker results in severely reduced traffic out of the ER, as measured by gel shift and the acquisition of endoH resistance in the wild-type channel (data not shown). The N-terminal fusion resulted in free GFP and consequently was not useful for our experiment. Although imaging of kinetics using fixed cells is more laborious and prone to error, we found that a large sample size and a rigid adherence to a short (<10 min) injection period made it possible to quantitatively measure a difference between wild-type and mutant channel.

There are two factors that could affect the accuracy of our measurements. First, the method of image analysis that we have employed makes the assumption that all non-Golgi fluorescence in the cell can be attributed to Shaker that has not as yet trafficked to the Golgi (i.e., Shaker that is at a pre-Golgi location in the secretory pathway). This assumption is likely to be inaccurate. Specifically, there is most probably some Shaker on the cell surface at all times measured, resulting both from delivery during the initial 2 h expression period, when the cells are incubated at 37 °C, and during the 0−4 h traffic period, at 20 °C. This would underestimate the Golgi fraction for both wild-type and mutant Shaker, at all times. However, biotinylation experiments suggest that wild-type Shaker traffics faster than the mutant. Thus, the measured wild-type Golgi fraction is likely to be a greater underestimation than the mutant fraction. If anything, therefore, the differences between the mutant and wild-type transport rates are likely to be greater than those observed here. We have tried to quantify the surface fraction in an imaging experiment using an engineered extracellular FLAG tag, but these experiments have been unsuccessful. Although this approach was used previously to map the topology of Shaker expressed in Xenopus oocytes (*5*), we were unable to visualize the FLAG-tagged channel either in unpermeabilized or in permeabilized mammalian cells. Second, if the two channels are degraded at different rates from an intracellular location, this could affect our measurement of the Golgi fraction. However, there is no difference in wild-type and mutant channel stability at 20 °C in HeLa cells.

We cannot formally distinguish between an effect of glycosylation on retrograde Golgi-to-ER traffic as compared to forward (ER-to-Golgi) traffic through the secretory pathway. Also, it is possible that there is a difference between mutant and wild-type channel in terms of their Golgi-plasma membrane transport rates. A similar imaging experiment to compare these rates, although theoretically feasible, is complicated by the fact that the two channels differ markedly in the extent to which traffic out of the ER occurs, even after 4−5 h at 20 °C. This makes quantitative interpretation of a "Golgi exit" experiment difficult. More importantly, inhibition of Golgi glycosylation enzymes seems to have little effect on the transport of a number of proteins (*48*, *49*). In sum, the mutant unglycosylated Shaker channel is transported more slowly from ER to Golgi than the wild type at 20 ˚C, although we do not know if this difference persists at 37 ×bcC. Given the relatively rapid passage of proteins through the Golgi apparatus, an actual measurement is not possible at the higher temperature. Different rates of ER-to-Golgi transport may contribute at least partially to the difference in rate of delivery of the two channels to the cell surface.

One obvious explanation for slowed ER export of unglycosylated Shaker is that the absence of the carbohydrate moiety results in a reduced rate of productive folding, slower acquisition of an export-competent conformation, and, consequently, slower ER export. Glycosylation could affect folding rate directly by enhancing the stability of the correctly folded state, as has been demonstrated in studies on several proteins and peptides in vitro (*50*−*52*). Alternatively, but not exclusively, the effect of glycosylation could be indirect, via interaction with a chaperone. The obvious candidate for the latter role is the lectin-like chaperone calnexin, which is important for the folding of a large number of membrane glycoproteins (*20*). It has been shown to interact transiently with Shaker in a glycosylation-dependent manner (*9*). Treatment with castanospermine, by inhibiting ER glucosidase I activity, blocks interaction of calnexin with most substrates. In preliminary experiments, we have observed little effect of castanospermine on the rate of surface delivery of the Shaker channel, making it likely that the glycosylation effect in our experiments is not calnexin-dependent. This does not rule out a role for the chaperone (or the lumenal lectin calreticulin) in Shaker biogenesis, but it does indicate that such a role, if any, is not rate limiting in the glycosylation-dependent effect that we report here. Alternatively, this could merely be yet another example of redundancy in ER chaperone function, as has been previously demonstrated (*16*, *53*−*57*). It is also possible that there are other glycosylation-dependent chaperones that promote either folding or export of the Shaker channel. For instance, the mannose-binding lectin ERGIC53 has been implicated in the ER-to-Golgi transport of glycoproteins such as coagulation factors V and VIII (*58*−*61*) and human cathepsin Z (*62*). It is not known whether ERGIC 53 interacts with Shaker, but it is conceivable that it, or some other unidentified ER-to-Golgi transport factor, affects ER export of Shaker in a glycosylation-dependent manner.

It remains to be seen whether the difference in traffic rates reported here also holds true in a more homologous system (i.e., for Shaker in insect cells or Kv1 channels in mammalian cells). Although there are clearly differences in complex carbohydrate processing between insect and mammalian cells (*63*, *64*), the $Glu_3Man_9GlcNac_2$ carbohydrate moiety that is added on to the nascent protein in the ER is identical in both systems (*65*, *66*). Consequently, it is reasonable to assume that glycosylation-mediated effects on folding in the ER are similar. Also, the sequence homology between Drosophila and mammalian Kv1 channels is quite high (about 76% identity in the core region) (*67*), and Drosophila is known to possess the components of the lectin-based quality control system (*68*−*71*). Nevertheless, it is important that further studies include experiments in more homologous systems. This is further underscored by the possibility that experiments done in heterologous systems generate results that vary with cell type.

Since the activity of an excitable cell is determined by the type and number of ion channels on its surface, factors that affect one or other of these parameters would be expected to play a role in overall cell physiology (*1*, *72*). Recent experiments demonstrate that channel surface levels can be controlled by specific signals that affect channel traffic (*73*−*77*), thus providing further support for the idea that

regulation of traffic steps may be a mechanism for tuning the surface channel profile for a given cell type or developmental stage (*78*, *79*). For the voltage-gated potassium channels, residues in the cytosolic carboxyl terminus (*73*) as well as at the external face of the pore itself (*80*, *81*) have been implicated in efficient traffic out of the ER. Glycosylation does not fall into the category of a specific signal that is amenable to regulation, and it is clearly not absolutely required for export from the ER. However, the fact that glycosylation contributes to the overall rate of this traffic step and, perhaps consequently, affects channel surface levels (albeit only in certain cell types) underscores its relevance for cell physiology. Further experiments are needed to directly address whether the effect of glycosylation on Shaker secretory traffic results in pathology in the organism.

ACKNOWLEDGMENT

We are grateful to J. Rothman for the anti-GOS 28 antibody and to D. Papazian for the plasmid encoding N259Q+N263Q mutant Shaker and to Yu Chen for writing the imaging software. NdS would like to thank G. Kreitzer for help with microinjection, as well as J. Schmoranzer, T. Sakmar, M. Goulian, and D. Peter for many helpful discussions.

REFERENCES

1. Hille, B. (1984) *Ionic Channels Of Excitable Membranes*, Sinauer Associates Inc., Sunderland, MA.
2. Trimmer, J. S. (1998) *Curr. Opin. Neurobiol. 8*, 370−374.
3. Schulteis, C. T., Nagaya, N., and Papazian, D. M. (1996) *Biochemistry 35*, 12133−12140.
4. MacKinnon, R. (1991) *Nature 350*, 232−235.
5. Shih, T. M. and Goldin, A. L. (1997) *J. Cell Biol. 136*, 1037−1045.
6. Papazian, D. M. (1999) *Neuron 23*, 7−10.
7. Nagaya, N. and Papazian, D. M. (1997) *J. Biol. Chem. 272*, 3022−3027.
8. Deal, K. K., Lovinger, D. M., and Tamkun, M. M. (1994) *J. Neurosci. 14*, 1666−1676.
9. Nagaya, N., Schulteis, C. T., and Papazian, D. M. (1999) *Receptors. Channels 6*, 229−239.
10. Schulteis, C. T., Nagaya, N., and Papazian, D. M. (1998) *J. Biol. Chem. 273*, 26210−26217.
11. Rosenberg, R. L. and East, J. E. (1992) *Nature 360*, 166−169.
12. Kornfeld, R. and Kornfeld, S. (1985) *Annu. Rev. Biochem. 54*, 631−664.
13. Nilsson, I. M. and von Heijne, G. (1993) *J. Biol. Chem. 268*, 5798−5801.
14. Silberstein, S. and Gilmore, R. (1996) *FASEB J. 10*, 849−858.
15. Helenius, A. and Aebi, M. (2001) *Science 291*, 2364−2369.
16. Hammond, C., Braakman, I., and Helenius, A. (1994) *Proc. Natl. Acad. Sci. U.S.A 91*, 913−917.
17. Ware, F. E., Vassilakos, A., Peterson, P. A., Jackson, M. R., Lehrman, M. A., and Williams, D. B. (1995) *J. Biol. Chem. 270*, 4697−4704.
18. Spiro, R. G., Zhu, Q., Bhoyroo, V., and Soling, H. D. (1996) *J. Biol. Chem. 271*, 11588−11594.
19. Hebert, D. N., Foellmer, B., and Helenius, A. (1995) *Cell 81*, 425−433.
20. Parodi, A. J. (2000) *Annu. Rev. Biochem. 69*, 69−93.
21. Trombetta, S. E. and Parodi, A. J. (1992) *J. Biol. Chem. 267*, 9236−9240.
22. Liu, Y., Choudhury, P., Cabral, C. M., and Sifers, R. N. (1999) *J. Biol. Chem. 274*, 5861−5867.
23. Cabral, C. M., Choudhury, P., Liu, Y., and Sifers, R. N. (2000) *J. Biol. Chem. 275*, 25015−25022.
24. Jakob, C. A., Burda, P., Roth, J., and Aebi, M. (1998) *J. Cell Biol. 142*, 1223−1233.
25. Su, K., Stoller, T., Rocco, J., Zemsky, J., and Green, R. (1993) *J. Biol. Chem. 268*, 14301−14309.
26. Gehle, V. M., Walcott, E. C., Nishizaki, T., and Sumikawa, K. (1997) *Brain Res. Mol. Brain Res. 45*, 219−229.
27. Ramanathan, V. K. and Hall, Z. W. (1999) *J. Biol. Chem. 274*, 20513−20520.
28. Kaushal, S., Ridge, K. D., and Khorana, H. G. (1994) *Proc. Natl. Acad. Sci. U.S.A. 91*, 4024−4028.
29. Tifft, C. J., Proia, R. L., and Camerini-Otero, R. D. (1992) *J. Biol. Chem. 267*, 3268−3273.
30. Albrecht, B., Woisetschlager, M., and Robertson, M. W. (2000) *J. Immunol. 165*, 5686−5694.
31. Hawtin, S. R., Davies, A. R., Matthews, G., and Wheatley, M. (2001) *Biochem. J. 357*, 73−81.
32. Davis, D. P., Rozell, T. G., Liu, X., and Segaloff, D. L. (1997) *Mol. Endocrinol. 11*, 550−562.
33. Zhou, Z., Gong, Q., Epstein, M. L., and January, C. T. (1998) *J. Biol. Chem. 273*, 21061−21066.
34. Dennis, J. W., Granovsky, M., and Warren, C. E. (1999) *Bioessays 21*, 412−421.
35. Manganas, L. N., Akhtar, S., Antonucci, D. E., Campomanes, C. R., Dolly, J. O., and Trimmer, J. S. (2001) *J. Biol. Chem. 276*, 49427−49434.
36. Santacruz-Toloza, L., Huang, Y., John, S. A., and Papazian, D. M. (1994) *Biochemistry 33*, 5607−5613.
37. Schulteis, C. T., John, S. A., Huang, Y., Tang, C. Y., and Papazian, D. M. (1995) *Biochemistry 34*, 1725−1733.
38. Khanna, R., Myers, M. P., Laine, M., and Papazian, D. M. (2001) *J. Biol. Chem. 276*, 34028−34034.
39. Liu, T. I., Lebaric, Z. N., Rosenthal, J. J., and Gilly, W. F. (2001) *J Neurophysiol. 85*, 61−71.
40. Shen, N. V., Chen, X., Boyer, M. M., and Pfaffinger, P. J. (1993) *Neuron 11*, 67−76.
41. Santacruz-Toloza, L., Perozo, E., and Papazian, D. M. (1994) *Biochemistry 33*, 1295−1299.
42. Lodish, H. F., Kong, N., Snider, M., and Strous, G. J. (1983) *Nature 304*, 80−83.
43. Hay, J. C., Klumperman, J., Oorschot, V., Steegmaier, M., Kuo, C. S., and Scheller, R. H. (1998) *J. Cell Biol. 141*, 1489−1502.
44. Orci, L., Ravazzola, M., Volchuk, A., Engel, T., Gmachl, M., Amherdt, M., Perrelet, A., Sollner, T. H., and Rothman, J. E. (2000) *Proc. Natl. Acad. Sci. U.S.A. 97*, 10400−10405.
45. Chandy, K. G. and Gutman, G. A. (1995) in *Handbook of Receptors and Channels* (North, R. A., Ed.) pp 1−71, CRC Press, Boca Raton, FL.
46. Zafra, F. and Gimenez, C. (2001) *Biochem. Soc. Trans. 29*, 746−750.
47. Scheiffele, P., Peranen, J., and Simons, K. (1995) *Nature 378*, 96−98.
48. Elbein, A. D. (1991) *FASEB J. 5*, 3055−3063.
49. Stanley, P. (1984) *Annu. Rev. Genet. 18*, 525−552.
50. Imperiali, B. and O'Connor, S. E. (1999) *Curr. Opin. Chem. Biol. 3*, 643−649.
51. Wormald, M. R. and Dwek, R. A. (1999) *Structure. Fold. Des. 7*, R155−R160.
52. Kern, G., Kern, D., Jaenicke, R., and Seckler, R. (1993) *Protein Sci. 2*, 1862−1868.
53. Braakman, I. and van Anken, E. (2000) *Traffic. 1*, 533−539.
54. Zhang, J. X., Braakman, I., Matlack, K. E., and Helenius, A. (1997) *Mol. Biol. Cell 8*, 1943−1954.
55. Gaudin, Y. (1997) *J. Virol. 71*, 3742−3750.
56. McGinnes, L. W. and Morrison, T. G. (1998) *Virus Res. 53*, 175−185.
57. Molinari, M. and Helenius, A. (2000) *Science 288*, 331−333.
58. Moussalli, M., Pipe, S. W., Hauri, H. P., Nichols, W. C., Ginsburg, D., and Kaufman, R. J. (1999) *J. Biol. Chem. 274*, 32539−32542.
59. Nichols, W. C., Terry, V. H., Wheatley, M. A., Yang, A., Zivelin, A., Ciavarella, N., Stefanile, C., Matsushita, T., Saito, H., de Bosch, N. B., Ruiz-Saez, A., Torres, A., Thompson, A. R., Feinstein, D. I., White, G. C., Negrier, C., Vinciguerra, C., Aktan, M., Kaufman, R. J., Ginsburg, D., and Seligsohn, U. (1999) *Blood 93*, 2261−2266.
60. Neerman-Arbez, M., Johnson, K. M., Morris, M. A., McVey, J. H., Peyvandi, F., Nichols, W. C., Ginsburg, D., Rossier, C., Antonarakis, S. E., and Tuddenham, E. G. (1999) *Blood 93*, 2253−2260.
61. Nichols, W. C., Seligsohn, U., Zivelin, A., Terry, V. H., Hertel, C. E., Wheatley, M. A., Moussalli, M. J., Hauri, H. P., Ciavarella, N., Kaufman, R. J., and Ginsburg, D. (1998) *Cell 93*, 61−70.

62. Appenzeller, C., Andersson, H., Kappeler, F., and Hauri, H. P. (1999) *Nat. Cell Biol. 1*, 330−334.
63. Jarvis, D. L. and Finn, E. E. (1996) *Nat. Biotechnol. 14*, 1288−1292.
64. Jarvis, D. L. and Finn, E. E. (1995) *Virology 212*, 500−511.
65. Hsieh, P. and Robbins, P. W. (1984) *J. Biol. Chem. 259*, 2375−2382.
66. Jarvis, D. L. and Garcia, A., Jr. (1994) *Virology 205*, 300−313.
67. Wei, A., Covarrubias, M., Butler, A., Baker, K., Pak, M., and Salkoff, L. (1990) *Science 248*, 599−603.
68. Smith, M. J. (1992) *DNA Seq. 3*, 247−250.
69. Parker, C. G., Fessler, L. I., Nelson, R. E., and Fessler, J. H. (1995) *EMBO J. 14*, 1294−1303.
70. Christodoulou, S., Lockyer, A. E., Foster, J. M., Hoheisel, J. D., and Roberts, D. B. (1997) *Gene 191*, 143−148.
71. Ziak, M., Meier, M., Etter, K. S., and Roth, J. (2001) *Biochem. Biophys. Res. Commun. 280*, 363−367.
72. Levitan, E. S. and Takimoto, K. (1998) *J. Neurobiol. 37*, 60−68.
73. Li, D., Takimoto, K., and Levitan, E. S. (2000) *J. Biol. Chem. 275*, 11597−11602.
74. Ma, D., Zerangue, N., Lin, Y. F., Collins, A., Yu, M., Jan, Y. N., and Jan, L. Y. (2001) *Science 291*, 316−319.
75. Zerangue, N., Schwappach, B., Jan, Y. N., and Jan, L. Y. (1999) *Neuron 22*, 537−548.
76. Sharma, N., Crane, A., Clement, J. P., Gonzalez, G., Babenko, A. P., Bryan, J., and Aguilar-Bryan, L. (1999) *J. Biol. Chem. 274*, 20628−20632.
77. Hough, E., Beech, D. J., and Sivaprasadarao, A. (2000) *Pflugers Arch. 440*, 481−487.
78. Manganas, L. N. and Trimmer, J. S. (2000) *J Biol. Chem. 275*, 29685−29693.
79. Al Awqati, Q. (1985) *Soc. Gen. Physiol Ser. 39*, 149−157.
80. Manganas, L. N., Wang, Q., Scannevin, R. H., Antonucci, D. E., Rhodes, K. J., and Trimmer, J. S. (2001) *Proc. Natl. Acad. Sci. U.S.A. 98*, 14055−14059.
81. Zhu, J., Watanabe, I., Gomez, B., and Thornhill, W. B. (2001) *J Biol. Chem. 276*, 39419−39427.

BI0258041